Homeostatic Scaling Requires Group I mGluR Activation Mediated by Homer1a

Jia-Hua Hu,[1,6] Joo Min Park,[1,6] Sungjin Park,[1,6] Bo Xiao,[1,5] Marlin H. Dehoff,[1] Sangmok Kim,[1] Takashi Hayashi,[1,2] Martin K. Schwarz,[4] Richard L. Huganir,[1,2] Peter H. Seeburg,[4] David J. Linden,[1] and Paul F. Worley[1,3,*]

[1]Solomon H. Snyder Department of Neuroscience
[2]Howard Hughes Medical Institute
[3]Department of Neurology
Johns Hopkins University School of Medicine, Baltimore, MD 21205, USA
[4]Department of Molecular Neurobiology, Max Planck Institute for Medical Research, 69120 Heidelberg, Germany
[5]The State Key Laboratory of Biotherapy, West China Hospital, Sichuan University, Chengdu, P.R. China, 610041
[6]These authors contributed equally to this work
*Correspondence: pworley@jhmi.edu
DOI 10.1016/j.neuron.2010.11.008

SUMMARY

Homeostatic scaling is a non-Hebbian form of neural plasticity that maintains neuronal excitability and informational content of synaptic arrays in the face of changes of network activity. Here, we demonstrate that homeostatic scaling is dependent on group I metabotropic glutamate receptor activation that is mediated by the immediate early gene Homer1a. Homer1a is transiently upregulated during increases in network activity and evokes agonist-independent signaling of group I mGluRs that scales down the expression of synaptic AMPA receptors. Homer1a effects are dynamic and play a role in the induction of scaling. Similar to mGluR-LTD, Homer1a-dependent scaling involves a reduction of tyrosine phosphorylation of GluA2 (GluR2), but is distinct in that it exploits a unique signaling property of group I mGluR to confer cell-wide, agonist-independent activation of the receptor. These studies reveal an elegant interplay of mechanisms that underlie Hebbian and non-Hebbian plasticity.

INTRODUCTION

Neurons maintain basic properties of excitability despite changes in synaptic input that naturally occur either because of Hebbian changes in synaptic strength or activity of the network of neurons that drive their firing (Turrigiano, 2008). One homeostatic adaptation involves a cell-wide increase or decrease of postsynaptic AMPAR at excitatory synapses. This process is thought to occur in a manner that maintains the relative strengths of synapses by effectively scaling all synapses by the same multiplicative factor (Turrigiano and Nelson, 2000). Homeostatic scaling can be modeled in primary neuronal cultures wherein the strength of synapses is scaled up by diminished network activity, or scaled down by increased network activity. Recent studies have provided insights into the molecular basis of homeostatic scaling. One mechanism involves the cellular immediate early gene (IEG) termed Arc (also termed Arg3.1). Consistent with its regulation as an IEG in vivo (Lyford et al., 1995), addition of bicuculline to cultures increases network activity and increases Arc protein expression (Shepherd et al., 2006). Arc is a cytosolic protein that interacts with endocytic proteins including endophilin2/3 and dynamin to enhance the rate of endocytosis of AMPAR (Chowdhury et al., 2006), and consequently its upregulation reduces synaptic AMPAR (Shepherd et al., 2006). This cell wide, postsynaptic mechanism is tuned to the physiological range of neuronal activities.

Studies of Arc also provide insight into how neurons can integrate Hebbian plasticity with homeostatic scaling. Acute activation of group I mGluRs on hippocampal or cortical neurons results in rapid and sustained depression of synaptic transmission (mGluR-LTD) by a mechanism that requires de novo translation of mRNAs (Snyder et al., 2001), including Arc (Park et al., 2008; Waung et al., 2008), and is mediated by accelerated endocytosis of surface AMPAR. De novo translation of Arc required for mGluR-LTD is dependent on elongation factor 2 kinase (eEF2K) activation, which can be regulated locally by synaptic activity. eEF2K is not required for Arc translation in response to growth factors or for delayed responses to mGluR activation, and homeostatic scaling is preserved in the eEF2K knockout (KO). Thus, differences in the translational regulation of Arc underlie its conditional contributions to homeostatic scaling versus mGluR-LTD. These observations highlight mechanistic similarities and differences between homeostatic scaling and mGluR-LTD.

In the present study, we report that group I mGluRs signaling plays an essential role in homeostatic scaling. The mechanism of activation of mGluR in homeostatic scaling is distinctly different than in mGluR-LTD, wherein Hebbian effects are mediated by local activation of the receptor by synaptically released glutamate. In homeostatic scaling, group I mGluRs activation is not due to glutamate acting on the receptor, but rather is due to the induction of the IEG Homer1a in the postsynaptic neuron, which creates a cell wide, agonist-independent activation of mGluR. Homer1a binds a consensus proline rich sequence (PPXXF) present in the C terminus of group I metabotropic glutamate receptors (mGluR), and disrupts the crosslinking action of constitutively expressed forms of Homer (Brakeman et al., 1997;

Tu et al., 1998). Interruption of Homer crosslinking can activate the mGluR in the absence of glutamate (Ango et al., 2001), and this mechanism appears central to the action of Homer1a in homeostatic scaling. Studies further reveal Homer1a-dependent scaling is not dependent on Arc, but rather is linked to a reduction of the tyrosine phosphorylation of the AMPAR subunit GluA2 (GluR2). Changes in tyrosine phosphorylation of GluA2 have previously been implicated in insulin-dependent LTD (Ahmadian et al., 2004) and mGluR-LTD (Gladding et al., 2009). The involvement of regulated tyrosine phosphorylation of GluA2 in homeostatic scaling demonstrates a convergent molecular mechanism that may be differentially evoked either locally or cell-wide to produce Hebbian or non-Hebbian plasticity.

RESULTS

Agonist-Independent Activity of Group I mGluRs Is Required for Homeostatic Scaling

We examined the hypothesis that group I mGluR activity contributes to homeostatic scaling using antagonists of mGluR1 and mGluR5. The pharmacology of group I mGluR antagonists is notable in that it includes agents that competitively inhibit the glutamate binding pocket in the N terminus (O'Hara et al., 1993), as well as agents that noncompetitively bind within the transmembrane domain (Pagano et al., 2000). Noncompetitive agents can act as inverse agonists if they block agonist-independent activity, or as neutral antagonists if they do not block agonist-independent activity (Milligan, 2003). Days in vitro (DIV) 14 cortical neurons in culture were chronically treated with bicuculline (bic, 40 μM) in the presence or absence of group I mGluR antagonists, and scaling of AMPARs was monitored by surface biotinylation and immunohistochemistry (IHC). As expected, chronic bicuculline treatment reduced the levels of GluA1 (GluR1) and GluA2/3 (GluR2/3) on the cell surface. Inhibition of mGluR1 and mGluR5 with inverse agonists Bay 36-7620 (Bay, 10 μM) and 2-methyl-6-(phenylethynyl)-pyridine (MPEP, 5 μM) prevented the effect of bicuculline to reduce surface GluA1 and GluA2/3 (Figures 1A and 1B). Figure 1A illustrates a representative western blot at a single exposure, while quantitative data (Figure 1B) were obtained from additional exposures to assure signals were in the linear range. (The same approach is used for western data in all figures.) A similar effect was observed with the structurally different mGluR1 inverse agonist, LY367385 (LY, 100 μM) (Pula et al., 2004), together with MPEP (Figures 1A and 1B). Single treatment with Bay, LY, or MPEP did not prevent bicuculline-induced downregulation of surface AMPAR (data not shown), indicating that inhibition of both mGluR1 and mGluR5 is required. Competitive or neutral antagonists of group I mGluR did not block bicuculline-induced downregulation of GluA1 and GluA2/3 as shown by inhibition of mGluR1 with the neutral antagonist CPCCOEt (CP, 100 μM), and mGluR5 with the competitive antagonist (S)-MCPG (500 μM) (Figures 1A and 1B). This combination was verified to block the effect of group I mGluR signaling on ERK phosphorylation to a similar extent as Bay and MPEP (Figures S1A and S1B available online). CP (100 μM) combined with higher dose (S)-MCPG (2.5 mM) also failed to block bicuculline-induced downregulation of GluA1 and GluA2/3 (Figures S1C and S1D).

Bay and MPEP, but not CP and MCPG, prevented bicuculline-evoked downregulation of surface GluA1 and GluA2 staining (Figures 1C and 1D). Competitive blockade of group I and group II mGluRs with the LY341495 (100 μM) (Kingston et al., 1998) also failed to prevent bicuculline-induced downregulation of surface GluA1 and GluA2/3 (Figures S1C and S1D).

The failure of CP and MCPG or LY341495 to block scaling to bicuculline suggests that mGluR activation is not due to glutamate released at synapses or glutamate that might accumulate in the medium. To further examine this issue, we added glutamate-pyruvate transaminase (GPT) to the medium during chronic bicuculline treatment at a concentration reported to prevent local accumulation of glutamate at synapses (Matthews et al., 2000; Pula et al., 2004). The K_d of GPT for glutamate is ~8 μM and this is close to the measured level of glutamate in the medium of our cultures (~7 μM). GPT did not alter the effect of chronic bicuculline to downregulate surface GluA1 and GluA2/3 (Figures S1E and S1F).

Effects of group I mGluR antagonists on bicuculline-evoked scaling were examined in parallel using electrophysiological recordings. Chronic treatment with Bay and MPEP produced an increase in the miniature excitatory postsynaptic current (mEPSC) amplitudes (control 20.9 ± 1.1 pA; n = 24 cells versus Bay/MPEP 26.7 ± 1.9 pA; n = 21 cells; [#]p < 0.05), and blocked the effect of bicuculline (bic 14.1 ± 0.2 pA; n = 28 cells versus bic/Bay/MPEP 25.7 ± 2.0 pA; n = 18 cells) (Figures 1E and 1F). By contrast, chronic CP and MCPG did not block the effect of bicuculline (amp: 13.5 ± 0.4 pA, **p < 0.01; frequency: 22.8 ± 2.6 Hz, n = 22 cells), and did not produce an increase in the basal mEPSC amplitude (21.8 ± 0.9 pA, n = 11 cells, Figures 1E and 1F) or frequency (22.0 ± 2.8 Hz, n = 11 cells). The cumulative histogram of mEPSCs indicates that Bay 36-7620 and MPEP produced a multiplicative increase of amplitudes, suggesting the antagonists produce a scaling up of relative synaptic weights (Turrigiano and Nelson, 2000). Chronic Bay and MPEP also increased the frequency of mEPSCs (control 23.4 ± 2.6 Hz; n = 24 cells versus Bay/MPEP 36.4 ± 4.4 Hz; n = 21 cells; [#]p < 0.05). This is consistent with either a presynaptic action of group I mGluRs or the possibility that Bay and MPEP convert silent synapses to active synapses.

Homer1a Scales AMPA Receptors and Is Dependent on Group I mGluRs

To assess if Homer1a can activate group I mGluRs in cortical neurons to downregulate surface AMPARs, we expressed Homer1a transgene by Sindbis virus infection for 24 hr, and assayed surface AMPARs by biotinylation and IHC. We compared effects of Homer1a with that of Arc (Shepherd et al., 2006). Neurons were treated with tetrodotoxin (TTX, 1 μM) to reduce native expression of Homer1a and Arc, and thereby isolate the action of the transgenes. Surface GluA1 and GluA2/3 were reduced in neurons that expressed Homer1a or Arc, compared to GFP (Figures 2A and 2B). Notably, Bay and MPEP blocked the action of Homer1a to downregulate AMPARs, but did not block the effect of Arc (Figures 2A and 2B). IHC confirmed that Homer1a or Arc expression reduces surface GluA1 and GluA2 expression. Bay and MPEP blocked the action of Homer1a, but not the action of Arc (Figures 2C–2F), suggesting
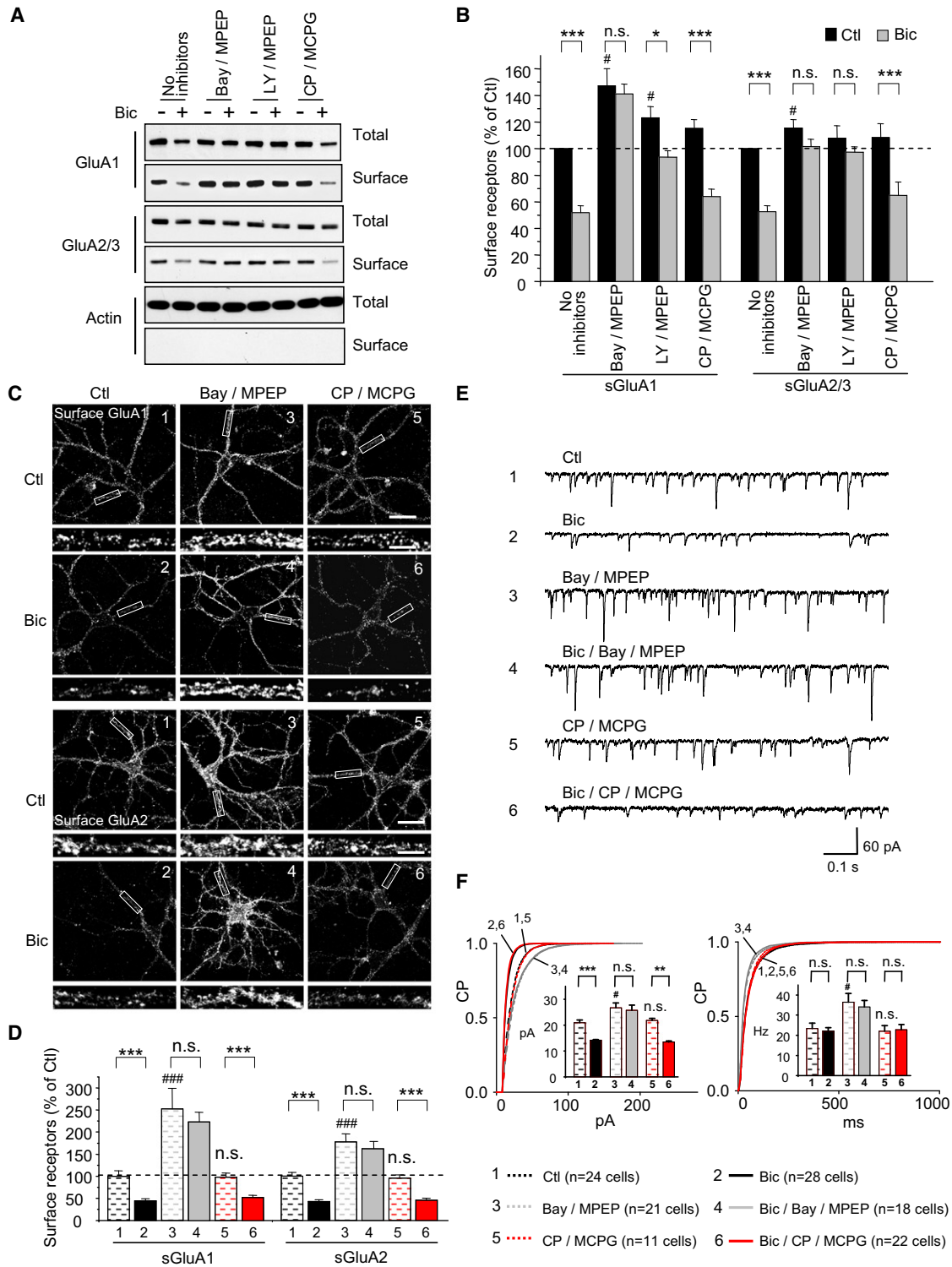
Figure 1. Group I mGluR Inverse Agonists Block Homeostatic Scaling of AMPARs

(A and B) Western blot and quantification of DIV14 cortical neurons treated with bicuculline (40 μM, 48 hr) and assayed for surface expression of AMPARs. Bicuculline reduced surface GluA1 and GluA2/3. Coapplication of inverse agonists of mGluR1 (Bay 36-7620; 10 μM) and mGluR5 (MPEP, 5 μM) or LY367385 (100 μM) together with MPEP blocked bicuculline effect, whereas the neutral antagonists CPCCOEt (100 μM) and (S)-MCPG (500 μM) did not. n = 5–12 for each group; *p < 0.05, ***p < 0.001 versus no bicuculline-treated control; #p < 0.05 versus no treatment control; n.s.: no significance; Bic: bicuculline; Bay: Bay 36-7620; LY: LY367385; CP: CPCCOEt in this and all subsequent figures.

that Homer1a acts upstream of group I mGluR while Arc acts downstream.

Generation of Homer1a-Specific Knockout Mice

We generated gene-targeted mice carrying a modified Homer1 allele that selectively prevents the expression of immediate-early gene forms of Homer1 including Homer1a and Ania3 (termed Homer1a KO; Figures S2A–S2D and Experimental Procedures). Homer1b/c, 2, and 3 protein expression is not changed in Homer1a KOs when compared with wild-type (WT) (Figure S2E). Similarly, expression of glutamate receptors mGluR1, mGluR5, GluA1, GluA2/3, and NR1 is not altered in Homer1a KO brains (Figure S2E). Homer1a KO mice are fertile, born at Mendelian frequency, and do not display obvious anatomical abnormalities. Maximal electroconvulsive seizure (MECS) induced Homer1a protein in WT mice, but not in Homer1a KO mice, and MECS did not alter Homer1b/c expression in either WT or Homer1a KO mice (Figure S2F).

Synaptic AMPARs Are Upregulated in Homer 1a KO Neurons in Culture

IHC and surface biotinylation assays revealed GluA1 and GluA2 are elevated on the surface of Homer1a KO neurons prepared from E18 cortex and cultured 14 DIV (Figures 3A–3D), whereas total levels of GluA1 and GluA2/3 were not different from WT neurons (Figures 3C and 3D). Surface mGluR5 is also significantly increased on Homer 1a KO neurons (Figures 3C and 3D). Whole cell recordings of pyramidal neurons confirm an increase in the average amplitude of mEPSCs in Homer1a KO neurons (28.9 ± 1.3 pA; n = 33 cells; Figure 3E) compared to WT neurons (20.9 ± 1.1 pA; n = 24 cells; ***p < 0.001), and indicate the increase is distributed over the entire range of recorded events consistent with scaling (Figure 3E). There was no difference in the frequency between WT (23.4 ± 2.6 Hz; n = 24 cells) and Homer1a KO neurons (25.3 ± 2.9 Hz; n = 33 cells; Figure 3E).

Homer 1a Transgene Reverses the Increase of AMPA Receptors in Homer1a KO Neurons

We asked whether Homer1a expression would rescue the phenotype of Homer1a KO neurons of increased synaptic AMPAR. To mimic the dynamic increase of Homer1a that occurs with IEG expression, we used Sindbis virus infection for 14–18 hr. We noted that mEPSCs recorded from Sindbis virus-expressing neurons were generally less than noninfected neurons of the same DIV, perhaps due to effect of Sindbis to usurp host cell protein translation (Xiong et al., 1989). Accordingly, we compared Sindbis virus infected neurons expressing Homer1a

versus GFP. mEPSC amplitudes recorded from Homer1a KO neurons expressing Homer1a transgene (13.7 ± 0.5 pA; n = 10 cells; *p < 0.05; Figures 4A and 4B) were significantly smaller than those recorded from neurons expressing only GFP (18.4 ± 1.6 pA; n = 13 cells). The shift to lower mEPSC amplitudes due to Homer1a expression was multiplicative. There was no difference in the frequency of mEPSCs between Homer1a (13.8 ± 1.7 Hz; n = 10 cells) and GFP expression (18.6 ± 3.0 Hz; n = 13 cells; Figure 4C). Biotinylation assays confirmed that surface expression of GluA1, GluA2/3, and mGluR5 were significantly reduced in Homer1a KO neurons that expressed Homer1a transgene compared with GFP, whereas total levels of AMPARs and mGluR5 were unchanged (Figures 4D and 4E). Consistent with the action of Homer1a to compete with Homer1c, Homer1a expression reduced the coimmunoprecipitation (co-IP) of mGluR5 with Homer1c compared to GFP-expressing neurons (Figure 4F).

## Homer1a Contributes to Homeostatic Scaling of AMPA Receptors

We monitored Homer1a mRNA and protein in DIV 14 cortical neurons treated with TTX or bicuculline for 3 hr, 6 hr, 12 hr, 24 hr, and 48 hr (Figure 5A). Bicuculline produced a time-dependent increase that was maximum at 6hrs for mRNA and 12 hr for protein (each ~8-fold), and returned to basal levels at 48 hr. By contrast, TTX treatment reduced Homer1a mRNA ~5-fold by 24 hr and protein by ~4-fold at 48 hr.

To assess how Homer1a KO affects homeostatic scaling, we examined the surface levels of AMPARs after chronic TTX or bicuculline treatment. Biotinylation and IHC assays revealed an absence of homeostatic adaptations of GluA2/3 in Homer1a KO neurons (Figures 5B–5E). Homeostatic adaptations of GluA1 were significantly reduced in Homer 1a KO neurons, but not as strikingly disrupted as GluA2. Homeostatic adaptations of mGluR5 were not significantly different in Homer1a KO neurons.

Disruption of homeostatic scaling in Homer1a KO neurons was also evident in mEPSCs recordings (Figures 5F and 5G). In contrast to WT neurons where TTX resulted in an increase of mEPSC (WT-control 20.9 ± 1.1 pA; n = 24 cells; TTX-treated 30.1 ± 2.2 pA; n = 15 cells, ***p < 0.001), mEPSC amplitudes of TTX-treated Homer1a KO neurons (31.4 ± 2.6 pA; n = 20 cells) were not significantly greater than untreated Homer1a KO neurons (28.9 ± 1.3 pA; n = 33 cells) (Figure 5G). Similarly, chronic bicuculline treatment reduced mEPSC amplitudes in WT neurons (14.1 ± 0.2 pA; n = 28 cells; ***p < 0.001), but did not produce a significant decrease in mEPSC amplitudes in Homer1a KO neurons (27.2 ± 1.9 pA; n = 35 cells) compared to

(C and D) Immunocytochemistry and quantification of DIV14 cortical neurons treated with bicuculline (40 μM, 48 hr) and assayed for surface expression of GluA1 and GluA2. Bicuculline treatment downregulated surface GluA1 and GluA2. Coapplication of Bay/MPEP increased surface GluA1 and GluA2 expression, and prevented the bicuculline scaling. Coapplication of neutral antagonists CP/MCPG did not alter surface GluA1 and GluA2 or bicuculline scaling (scale bar represents 30 μm and 5 μm in magnified dendrites). n = 24; ***p < 0.001 versus no bicuculline-treated control; ###p < 0.001 versus no treatment control.
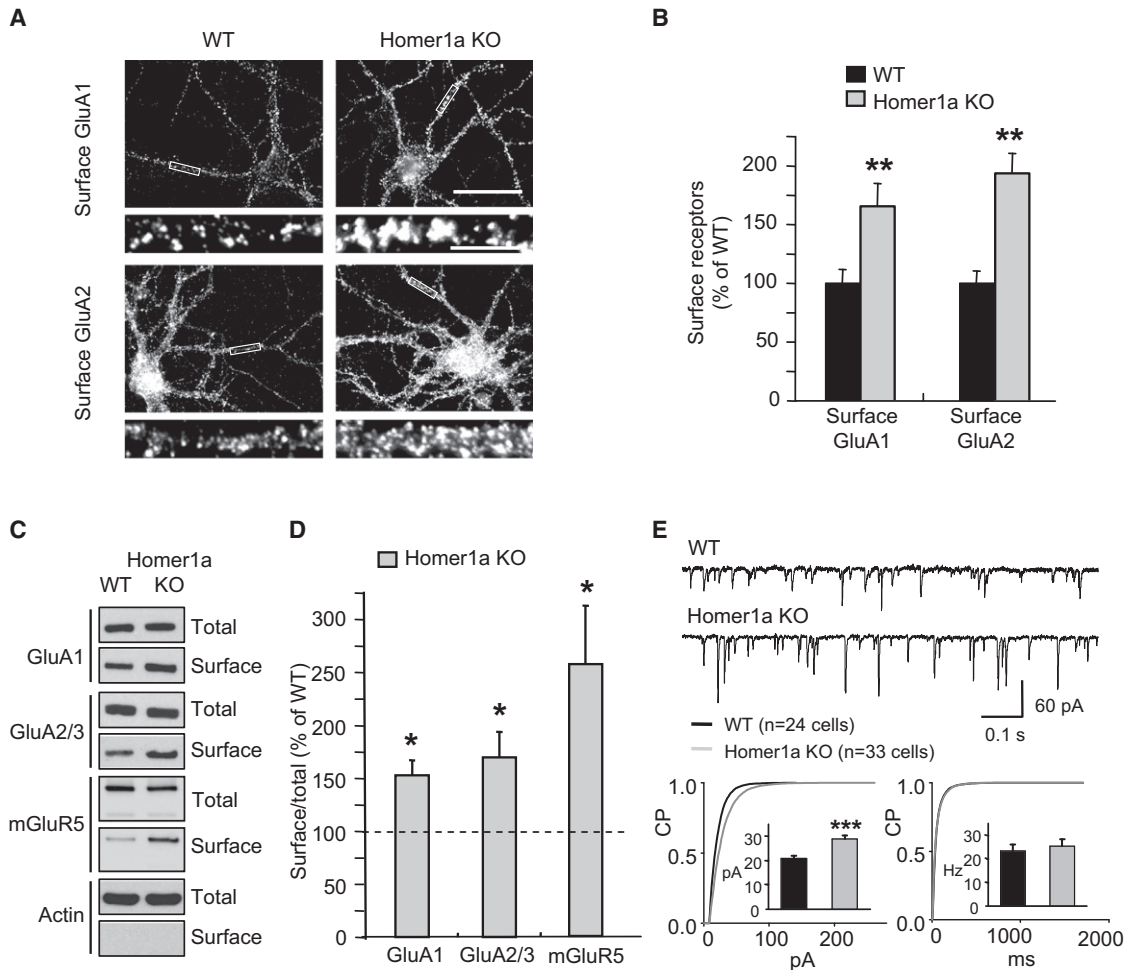
(E and F) Representative whole-cell recording traces and cumulative probability distribution of mEPSC amplitude or frequency from all events in control (n = 24 cells), Bic- (n = 28 cells), Bay/MPEP- (n = 21 cells), Bic/Bay/MPEP- (n = 18 cells), CP/MCPG- (n = 11 cells), and Bic/CP/MCPG- (n = 22 cells) treated neurons. Inset: bar graphs represent the mEPSC mean amplitude or frequency of each population. The effect of bic on mEPSC was blocked by group I mGluR inverse agonists, but not neutral antagonists. Neurons treated with Bay/MPEP showed an increase in both amplitude and frequency of mEPSCs. **p < 0.01, ***p < 0.001 versus no bicuculline-treated control; #p < 0.05 versus no treatment control. Statistical analysis conducted using one-way ANOVA with Bonferroni correction. Scale = 60 pA, 0.1 s.
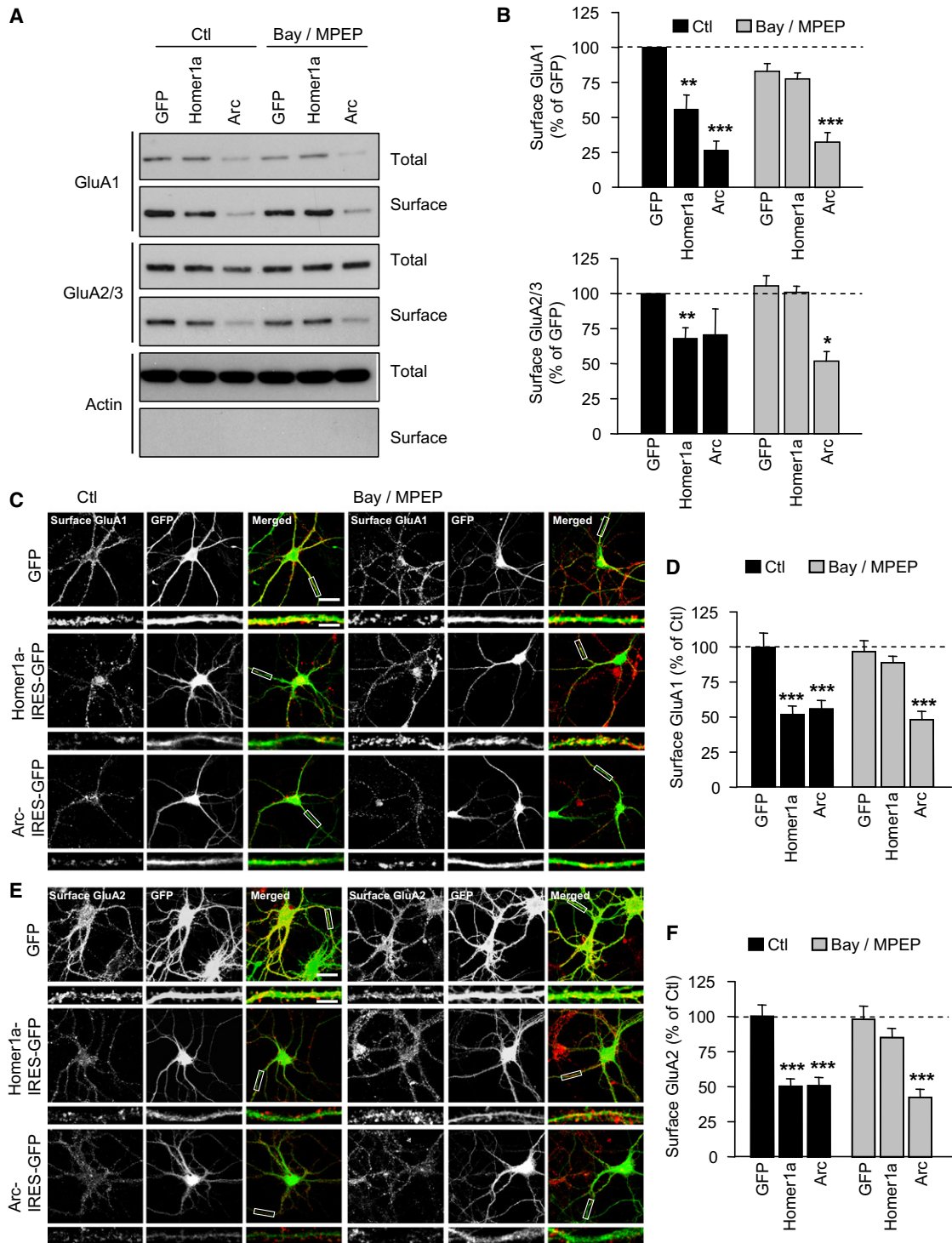
Figure 2. Homer1a Is an Upstream Regulator of Agonist-Independent Activity of Group I mGluRs

(A and B) Western blot and quantification demonstrating Homer1a or Arc transgene expression reduced surface GluA1 and GluA2. Bay/MPEP blocked the effect of Homer1a, but not Arc. n = 4; *p < 0.05, **p < 0.01, ***p < 0.001.

(C–F) Immunocytochemistry and quantification demonstrating Homer1a or Arc transgene expression reduced surface expression of GluA1 (C and D) and GluA2 (E and F), and coapplication of Bay/MPEP prevented Homer1a-induced, but not Arc-induced, effects (scale bar represents 30 μm and 5 μm in magnified dendrites). n = 12–24 each group; ***p < 0.001.

Figure 3. Synaptic AMPARs Are Elevated in Homer1a KO Neurons

(A and B) Representative immunocytochemistry and quantification of surface-labeled GluA1 and GluA2 on WT and Homer1a KO primary cortical neurons (scale bar represents 30 μm and 5 μm in magnified dendrites). n = 24 for each group; **p < 0.01.

(C and D) Western blots and quantification showed that surface GluA1, GluA2/3, and mGluR5 were increased on Homer1a KO neurons. n = 8 for each group; *p < 0.05.

(E) Representative whole-cell recording traces from WT and Homer1a KO neurons. Cumulative probability distribution of mEPSC amplitude or frequency in either control (n = 24 cells) or Homer1a KO (n = 33 cells). Inset: bar graphs represent the mEPSC mean amplitude or frequency of each population. mEPSC amplitudes were increased in Homer1a KO neurons (***p < 0.001). No change in frequency was observed.

untreated Homer1a KO neurons. Comparison of Homer1a KO neurons treated with bicuculline versus TTX suggested a small difference but was not statistically significant (27.2 ± 1.9 pA compared to 31.4 ± 2.6 pA; p = 0.19, not significant); this is dramatically different than WT neurons (14.1 ± 0.2 pA compared to 30.1 ± 2.2 pA). There was no difference in the frequency of mEPSCs between TTX-treated WT neurons (24.4 ± 2.6 Hz; n = 24 cells), bicuculline-treated WT neurons (22.2 ± 1.7 Hz; n = 28 cells), untreated WT neurons (23.4 ± 2.6 Hz; n = 24 cells), or similarly treated Homer1a KO neurons (TTX-treated, 24.9 ± 2.6 Hz; n = 20 cells; bicuculline-treated 27.6 ± 2.8 Hz; n = 35 cells; untreated 25.3 ± 2.9 Hz; n = 33 cells) (Figure 5G). These observations confirm that homeostatic changes of synaptic strength are markedly disrupted in Homer1a KO neurons. The modest

change of surface GluA1 detected in biochemical and IHC studies of Homer1a KO neurons is not manifest in electrophysiological data perhaps because GluA2 is the predominant receptor or the GluA1 that is scaled is extrasynaptic. Extrasynaptic pools of GluA1 have been described and implicated in synaptic plasticity (Makino and Malinow, 2009).

Chronic application of Bay and MPEP results in an increase of surface AMPAR and mEPSCs in WT neurons (Figure 1). If this increase reflects a block of the action of Homer1a that is expressed at steady state levels in neuronal cultures, it predicts that Bay and MPEP should not increase surface AMPAR in Homer1a KO neurons. This prediction was confirmed in both biochemical and electrophysiological assays (Figures S3A–S3D).
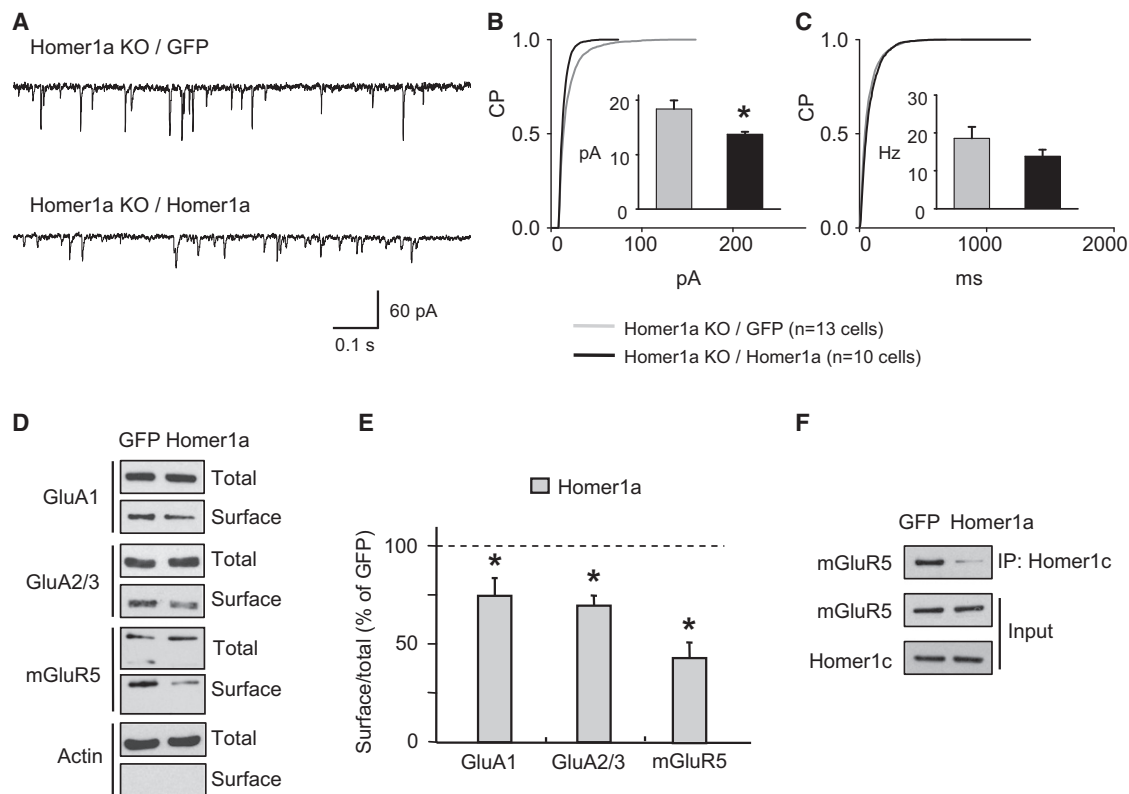
Figure 4. Homer1a Reduces Elevated Surface AMPARs and mGluR5 on Homer1a KO Neurons

(A–C) Whole cell recordings from Homer1a KO neurons infected with GFP or Homer1a Sindbis virus. Representative traces cumulative probability distribution of mEPSC amplitude or frequency. Inset: bar graphs represent the mEPSC mean amplitude or frequency of each population. Homer1a-expressing neurons (n = 10 cells) had significantly reduced mEPSC amplitudes compared to GFP neurons (n = 13) (*p < 0.05). No change in frequency was observed.

(D and E) Western blots and quantification demonstrating Homer1a transgene expression reduced surface expression of glutamate receptors (n = 4 each group; *p < 0.05) on Homer1a KO neurons.

(F) Homer1a transgene expression reduced mGluR5 co-IP with Homer1c from WT neurons.

Homer1a Scaling Does Not Require Arc

To assess how Homer1a downregulates surface AMPAR, we first considered the possibility that constitutive activation of group I mGluR would result in ongoing Arc translation. mGluR-receptor activation results in the rapid de novo translation of Arc and this is required for mGluR-LTD (Park et al., 2008; Waung et al., 2008), consistent with Arc's function to increase the rate of endocytosis of AMPAR (Chowdhury et al., 2006). However, Homer1a expressed in Arc KO cortical neurons by Sindbis virus resulted in downregulation of surface AMPAR identical to Homer1a's effect in WT neurons (Figures S4A and S4B). This observation indicates that the action of Homer1a is not dependent on Arc, and suggests that Homer1a and Arc function by independent pathways.

Homer1a Reduces GluA2 Tyrosine Phosphorylation

To assess the mechanism of Homer1a-dependent downregulation of surface AMPAR, we screened pharmacological agents for their ability to prevent effects of Homer1a expression by Sindbis virus on cortical neurons. Inhibition of tyrosine phosphatase by sodium orthovanadate (Na_3VO_4) prevented Homer1a-induced downregulation of AMPAR (Figure 6A). GluA2 is

phosphorylated on tyrosines in the C terminus, and reduction of tyrosine phosphorylation is linked to reduced surface expression (Ahmadian et al., 2004; Hayashi and Huganir, 2004). To examine this pathway, GluA2 was immunoprecipitated and blotted with phospho tyrosine Ab. Homer1a expression reduced GluA2 tyrosine phosphorylation (Figure 6B). Moreover, the effect of Homer1a to reduce GluA2 tyrosine phosphorylation was blocked by treatment of neurons with Bay and MPEP indicating that this action of Homer1a is dependent on group I mGluR signaling (Figure 6B). To explore the link between Homer and GluA2 tyrosine phosphorylation in vivo, we assayed cortex of WT and Homer1a KO mice. GluA2 tyrosine phosphorylation was increased in Homer1a KO cortex (Figure 6C). As a further test of this model, we examined Homer KO mice with genetic deletions of Homers 1, 2, and 3 (Homer TKO). Because these mice lack all Homer proteins, the model of Homer1a function that suggests it displaces long form Homer predicts that Homer TKO mice should mimic overexpression of Homer1a. Consistent with this prediction, tyrosine phosphorylation of GluA2 is markedly reduced (Figure 6D). Moreover, expression of GluA1 and GluA2/3 on the surface of Homer TKO cortical neurons in culture is reduced without changes in

total expression of these receptors (Figure 6E). Whole cell recordings of pyramidal neurons from layer II-III of acute cortical slices confirmed mEPSC amplitude from Homer TKO is decreased compared to WT (Figure 6F: Homer TKO 8.2 ± 0.2 pA; 9.7 ± 1.9Hz; n = 11 cells; WT 12.5 ± 1.4 pA; 9.8 ± 1.7Hz; n = 13 cells; **p < 0.01).

The acute effect of tyrosine phosphatase inhibitor Na_3VO_4 on mEPSC was examined in cortical neurons expressing Homer1a or GFP transgenes. Na_3VO_4 application increased mEPSC amplitude in Homer1a-expressing neurons, but not GFP-expressing neurons (Figure 6G). As a further test of the prediction that levels of surface AMPAR are reduced in Homer TKO mice due to a reduction of tyrosine phosphorylation, we monitored the mEPSC in acute cortical slices prepared from Homer TKO mice. Consistent with assays in cultures, addition of Na_3VO_4 to the perfusion buffer resulted in an increase of mEPSC in neurons from Homer TKO mice, but not WT mice (Figure 6H).

These data support a model in which constitutive group I mGluR activity, due to interruption of Homer binding, results in reduced GluA2 tyrosine phosphorylation and a consequent reduction of synaptic strength. As a further test of this model, we monitored the effect of acute blockade of group I mGluR activity, comparing Wt and Homer TKO neurons, with the expectation that reduced mEPSCs (Figure 6F) linked to reduced tyrosine phosphorylation is maintained by constitutive mGluR activity. Application of Bay (50 μM) and MPEP (10 μM) resulted in an acute increase of the mEPSC amplitude from neurons recorded in slices from Homer TKO mice, but not WT mice (Figure 6I).

Homer 1a Is Not Required for mGluR-LTD

The finding that homeostatic scaling is dependent on mGluR signaling suggests that homeostatic scaling may share mechanisms with mGluR-LTD. We first asked if mGluR-LTD is dependent on Homer1a using the acute hippocampal slice preparation. The mGluR5 agonist DHPG evoked robust LTD of the Schaffer-CA1 synapse that was monitored to 90 min, and was identical to WT mice (Figure S5A). Thus, Homer1a is not required for the induction or initial maintenance of mGluR-LTD.

Biculculline Scaling Occludes Chemical mGluR-LTD

We also examined how homeostatic scaling may impact mGluR-LTD by monitoring chemical LTD in cortical cultures after chronic bicuculline treatment. Acute treatment with DHPG (50 μM) resulted in robust downregulation of surface AMPAR in WT cortical neurons; however, DHPG treatment did not reduce surface AMPAR when added 48 hr after treatment with bicuculline (Figure S5B). Thus, bicuculline treatment evokes a downregulation of surface AMPARs that appears to occlude further reductions by DHPG treatment.

## Homer1a Contributes to the Induction of Scaling

The effect of acute application of Bay and MPEP to increase mEPSC in Homer TKO slices (Figure 6I) suggested this response may be useful to monitor the action of Homer1a. In WT neurons expressing Homer1a transgene, acute application of Bay and MPEP resulted in a gradual increase of mEPSC amplitude

(Figures 7A and 7B). This same phenomenon was detected in WT neurons 20–24 hr after the addition of bicuculline (Figure 7C and 7D), which parallels the time course of Homer1a protein induction (Figure 5A). Acute Bay and MPEP did not alter mEPSCs in WT neurons after 48 hr treatment of bicuculline (Figures S6A and S6B). These data suggest that Homer1a contributes to the induction of homeostatic scaling by enhancing mGluR activity, and this mechanism makes relatively less contribution to maintenance of scaling. In further support of this model, Bay and MPEP treatment, which blocks the scaling effect of bicuculline (Figure 1), does not reverse bicuculline scaling even if applied for an additional 48 hr after bicuculline (Figures S6C and S6D).

Homer 1a Scaling In Vivo

To examine Homer 1a scaling in vivo, we monitored responses of layer II-III pyramidal neurons in the acute cortical slices. As in culture, Homer1a KO pyramidal neurons had larger amplitude mEPSCs than WT neurons (Figures S7A and S7B: Homer1a KO 13.2 ± 0.8 pA; n = 7 cells; WT 10.4 ± 0.7 pA; n = 8 cells; *p < 0.05). There was no difference in mEPSC frequency between WT (14.9 ± 1.7 Hz; n = 8 cells) and Homer1a KO neurons (16.7 ± 3.8 Hz; n = 7 cells; Figures S7A and S7B). Acute application of Bay (50 μM) and MPEP (10 μM) to slices from naive WT or Homer1a KO mice did not change the amplitude of mEPSCs (not shown). To assess the contribution of activity-inducible Homer1a, we treated WT and Homer1a KO mice with MECS and prepared cortical slices 2 hr later. Slices were used for recordings 1–2 hr after preparation to correspond to the point of maximal expression of Homer1a protein after MECS (Brakeman et al., 1997). Homer1a mRNA was detected by in situ hybridization in ~13% of layer II-III cortical neurons in naive mice, and in ~35% of neurons in MECS treated mice (Figures S7C and S7D). Accordingly, we anticipated that effects of Homer1a might be evident in approximately one-third of randomly selected neurons. A comparison of mEPSC amplitudes in neurons from naive WT mice versus those treated with MECS showed a significant decrease in mEPSC amplitudes, whereas a similar comparison in Homer1a KO mice did not (Figure S7E). Bath application of Bay and MPEP increased the amplitude of mEPSCs in a subset of WT neurons (4/15) after MECS (Figures 7E and 7F). By contrast, bath application of Bay and MPEP did not result in an increase in mEPSC amplitude of neurons from Homer1a KO mice (0 of 16 neurons; different from WT neurons p < 0.05 using Fisher's exact test) (Figures 7E and 7F). To confirm the hypothesis that activity evokes constitutive mGluR signaling that reduces synaptic strength in WT mice, we employed a fos-GFP reporter mouse to identify living neurons that were activated by MECS (Barth et al., 2004). C-fos and *Homer1a* are coordinately induced in neurons by MECS (Barnes et al., 1994), and GFP was detected in approximately one-third of layer II-III pyramidal neurons after MECS. Bay and MPEP evoked a consistent increase of mEPSC recorded from GFP-expressing neurons after MECS (all neurons), but not from neurons lacking GFP (Figures 7G and 7H). These data are consistent with studies in neuronal cultures and support the hypothesis that neural activity in vivo evokes a reduction of mEPSC amplitude that is dynamically dependent on Homer1a and acutely reversed by inhibition of group I mGluR.
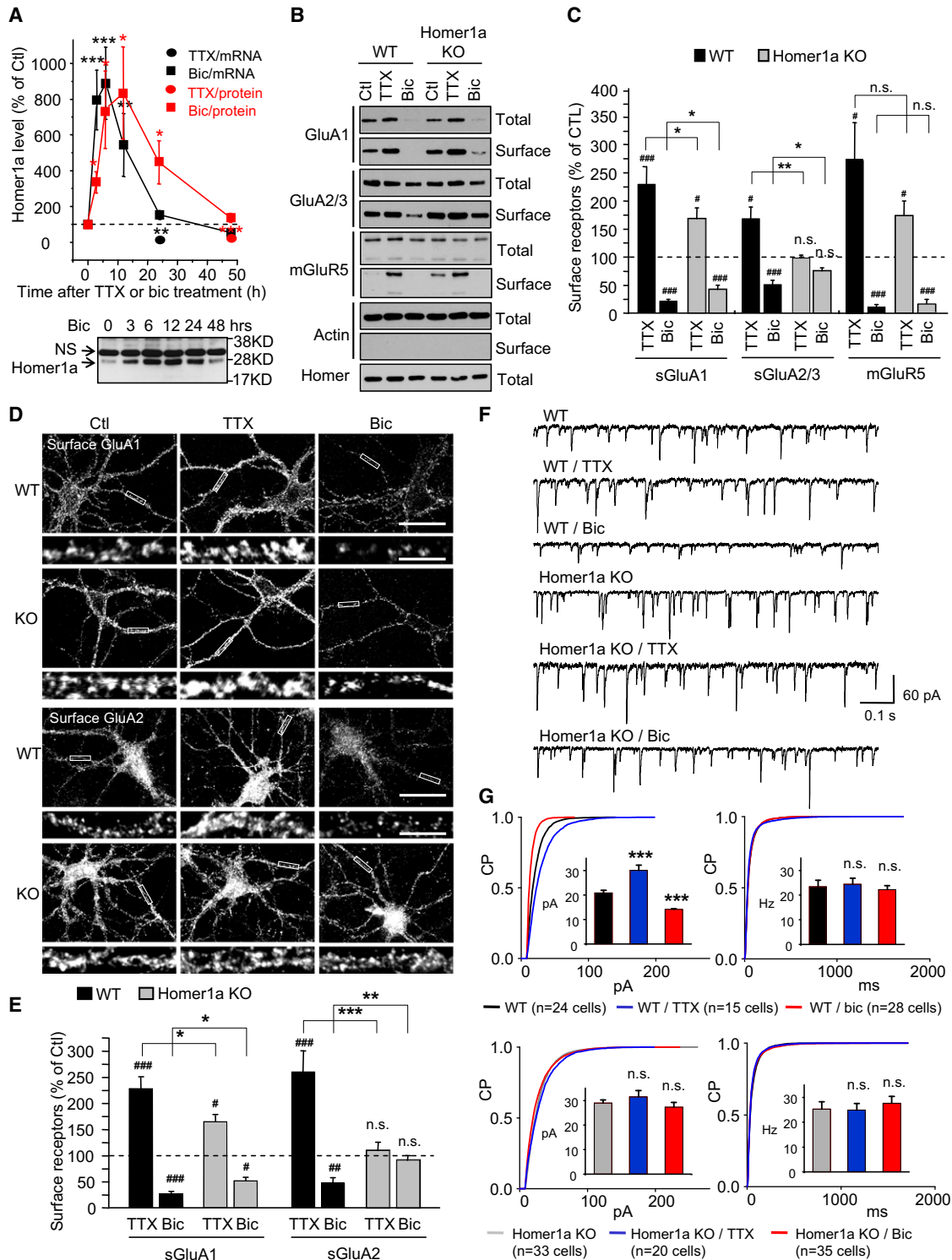
Figure 5. Homeostatic Scaling of AMPARs Is Impaired in Homer1a KO Neurons

(A) Real-time RT-PCR and immunoblot quantitation of Homer1a expression in primary cortical culture after chronic treatment with TTX or bicuculline. Bicuculline-induced Homer1a mRNA expression peaked 4–8 hr and returned to basal at 48 hr, whereas Homer1a protein peaked at 12 hr. n = 4 each group; *p < 0.05, ***p < 0.001. NS indicates a nonspecific band that reacts with Homer1a Ab.

(B and C) Western blots and quantification of glutamate receptors in WT and Homer1a KO cultured cortical neurons treated 48 hr with TTX (1 μM) or bicuculline (40 μM). Homer1a KO neurons underwent less scaling of GluA1 and GluA2/3. n = 8 each group; *p < 0.05, **p < 0.01 versus WT; #p < 0.05, ###p < 0.001 versus control; n.s., no significance.

DISCUSSION

Group I mGluR, Homer1a, and Homeostatic Scaling of AMPARs

Group I mGluR signaling in neurons encompasses a broad range of physiological outputs including dynamical control of Ca^{2+} release from intracellular stores (Feng et al., 2002; Tu et al., 1998; Yuan et al., 2003), Ca^{2+} influx via TRPC channels (Yuan et al., 2003), modulation of VSCC (Kitano et al., 2003), biosynthesis of phosphoinositides and cannabinoids (Maejima et al., 2001), regulation of protein synthetic pathways and activation of signaling kinases including ERK and PI3K (Park et al., 2008). Many of these outputs are coupled by Homer and are differentially altered by Homer1a (Kammermeier, 2008). The present study demonstrates that group I mGluRs play an essential role in homeostatic scaling of AMPAR. This represents a new function for mGluR signaling in neural plasticity, and reinforces the notion that Hebbian and non-Hebbian forms of plasticity can utilize shared pathways, albeit in ways that selectively modify individual synapses or cell-wide properties. mGluR signaling that mediates Hebbian forms of plasticity such as mGluR-LTD (Oliet et al., 1997) and spike-timing dependent plasticity (Dan and Poo, 2004) are driven by synaptically released glutamate and are localized to discrete regions of the dendrite. mGluR activity that drives homeostatic scaling is not dependent on glutamate acting at the receptor because scaling is not blocked by chronic treatment with competitive or neutral antagonists. Rather, mGluR activity that mediates scaling appears to be due to Homer1a disruption of the crosslinking activity of constitutively expressed long-form Homers, and occurs as a cell-wide response. The unique property of group I mGluR to signal in an agonist-independent mode that is controlled by an IEG creates an elegant mechanism to balance Hebbian and non-Hebbian plasticity.

Both Homer 1a and Arc contribute to homeostatic scaling, but appear to mediate independent pathways. Thus, Homer1a scaling is dependent on mGluR activity whereas Arc scaling is not. Moreover, Homer1a scaling is intact in Arc KO neurons. In contrast to Arc, which appears to be essential for both mGluR-LTD and homeostatic scaling, Homer1a appears to be selectively required for scaling because mGluR-LTD is intact in Homer1a KO hippocampus. The observation that mGluR signaling is modulated by an IEG and is essential for both Hebbian and non-Hebbian plasticity anticipates dynamical interactions between these forms of plasticity that are dependent on the activity history of the neuron. Our observation that scaling to chronic bicuculline prevents chemical LTD in cultured neurons provides an initial demonstration of this point.

The effect of Homer1a-dependent activation of mGluR can be revealed by acute increases of mEPSCs in response to inverse agonists. This effect is time-dependent and parallels the dynamical expression of Homer1a. Together with the observation that blockade of mGluR cannot reverse bicuculline-induced scaling once it is established suggest that Homer1a/mGluR are involved in the induction, but not the maintenance, of scaling. Although other mechanisms may contribute to agonist-independent signaling of group I mGluRs, such as phosphorylation dependent interruption of Homer multimerization (Brock et al., 2007; Mizutani et al., 2008), the phenotypic similarity of Homer1a KO neurons to WT neurons treated with group I mGluR inverse agonists suggests that Homer1a is the predominant regulator of agonist-independent signaling during homeostatic scaling.

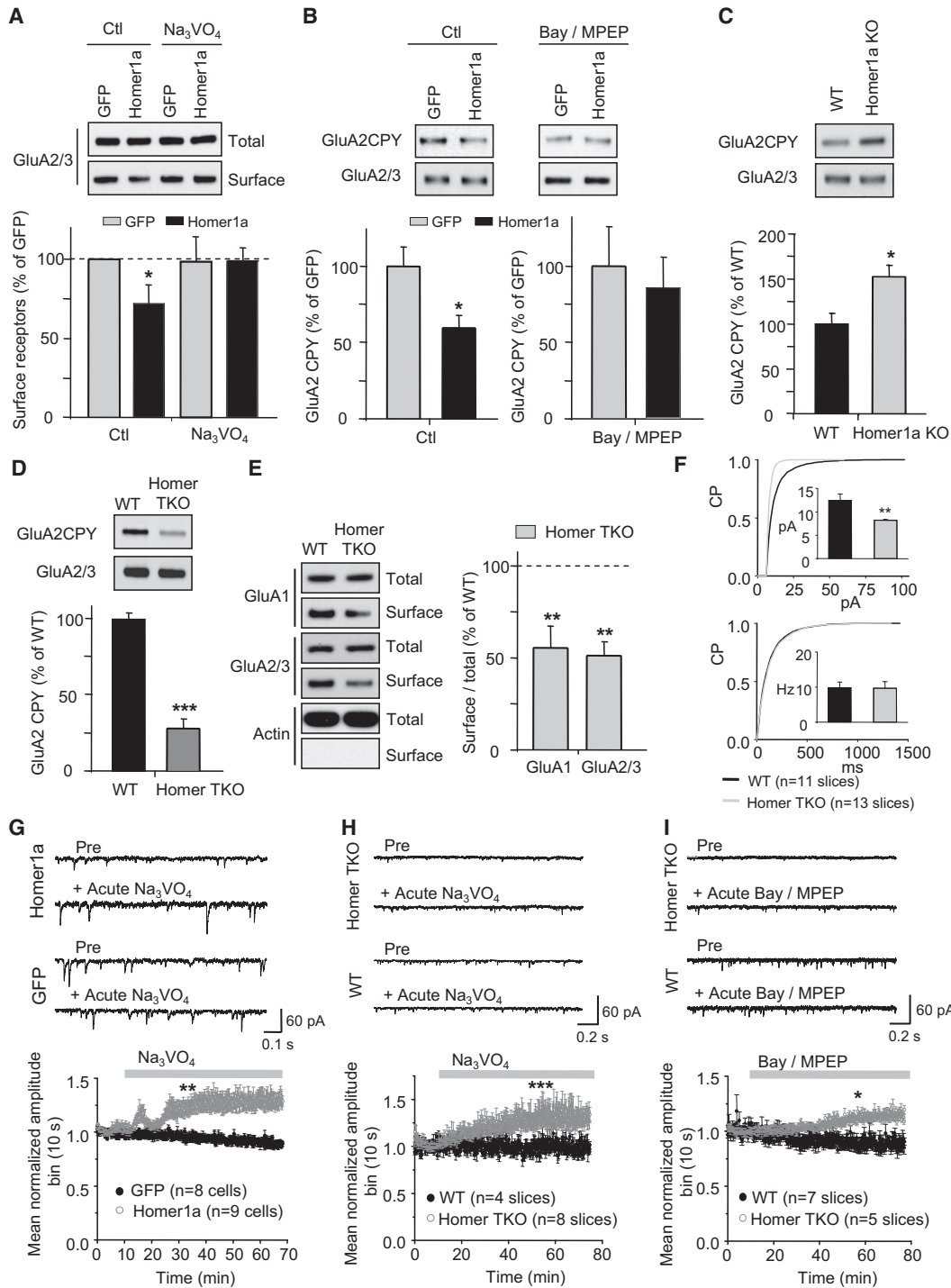### Homer Regulates the Tyrosine Phosphorylation of GluA2

Examination of the mechanism of Homer1a-dependent scaling revealed a role for Homer as a regulator of the tyrosine phosphorylation of GluA2. This effect is manifest after acute increases of Homer1a and is evident in vivo in both Homer1a KO and Homer TKO mice. The scaling effect of Homer1a transgene expression in cultured neurons is dependent on mGluR activity and all data are consistent with a canonical function of Homer1a. Thus, manipulations that interrupt Homer crosslinking, including Homer1a expression or deletion of all crosslinking forms of Homer (Homer TKO) result in reduced tyrosine phosphorylation of GluA2, whereas selective KO of Homer1a results in increased tyrosine phosphorylation. Inhibition of tyrosine phosphatase, which increases GluA2 tyrosine phosphorylation, prevents Homer1a-dependent downregulation of surface GluA2 and results in acute increases of synaptic strength in acute cortical slices of Homer TKO mice. Similar effects of tyrosine phosphatase inhibitors were noted on evoked synaptic responses in acute hippocampal slices (unpublished observation). GluA2 trafficking is linked to its tyrosine phosphorylation (Ahmadian et al., 2004; Hayashi and Huganir, 2004), and mGluR-LTD has been linked to de novo translation of the tyrosine phosphatase STEP (Zhang et al., 2008). The molecular basis of regulated tyrosine phosphorylation of GluA2 in scaling remains to be explored.

Homer 1a and Homeostatic Changes in Surface mGluR5

Surface expression of mGluR5 is increased by chronic treatment with TTX and reduced by chronic treatment with bicuculline, in a manner that parallels homeostatic changes in AMPAR (Figure 5). Homer1a may play a role in this process because surface mGluR5 is increased on Homer1a KO neurons, and Homer1a transgene expression downregulates surface mGluR5 (Figure 4). These effects contrast with previous studies in which Homer1a transgene expression increased surface mGluR5 (Ango et al., 2002). Differences in the duration of Homer1a expression may underlie this disparity. Importantly, scaling of surface mGluR5 is not significantly different in Homer1a KO neurons compared

(D and E) Representative immunohistochemistry and quantification of surface GluA1 and GluA2 in WT and Homer1a KO cortical neurons treated for 48 hr with TTX or bicuculline. KO neurons exhibited impaired scaling (scale bar represents 30 μm and 5 μm in magnified dendrites). n = 11–24; *p < 0.05, ***p < 0.001 versus WT; #p < 0.05, ##p < 0.01, ###p < 0.001 versus control; n.s., no significance.

(F and G) Representative whole-cell recording traces and cumulative probability distributions of mEPSC amplitude and frequency from WT and Homer1a KO neurons after TTX (WT: n = 15 cells, KO: n = 20 cells) or bicuculline (WT: n = 28 cells, KO: n = 35 cells) treatment for 48 hr. Inset: bar graphs represent the mEPSC mean amplitude or frequency of each population. Although WT neurons showed the expected scaling of mEPSC amplitudes, Homer1a KO neurons showed no significant changes of mEPSC amplitudes or frequency. ***p < 0.001 versus no treatment control. Statistical analysis conducted using one-way ANOVA with Bonferroni correction, scale = 60 pA, 0.1 s.

Figure 6. Homer1a Reduces GluA2 Tyrosine Phosphorylation

(A) Western blots and quantification show that sodium orthovanadate (1 mM, Na_3VO_4) blocks the scaling effect of Homer1a [Sindbis virus (24 hr)] on GluA2/3. n = 5 each group; *p < 0.05 versus GFP control.

(B) Homer1a reduces GluA2 tyrosine phosphorylation, and is blocked by Bay/MPEP. n = 4–5 each group; *p < 0.05 versus GFP control.

(C) GluA2 tyrosine phosphorylation is elevated in the brain of Homer1a KO mice compared to WT mice. n = 4 each group; *p < 0.05 versus WT.

(D) GluA2 tyrosine phosphorylation is reduced in the brain of Homer TKO mice compared to WT mice. n = 4–5 each group; *p < 0.05 versus WT.

(E) Surface GluA1 and GluA2/3 are decreased in Homer TKO cortical neurons. n = 6 for each group, **p < 0.01.

(F) Cumulative probability distribution of mEPSC amplitude and frequency from pyramidal neurons of layer II-III prefrontal cortex in slices prepared from naive WT or Homer TKO mice. Inset: bar graphs represent the mEPSC mean amplitude or frequency. Homer TKO neurons had significantly smaller mEPSC amplitudes (**p < 0.01).
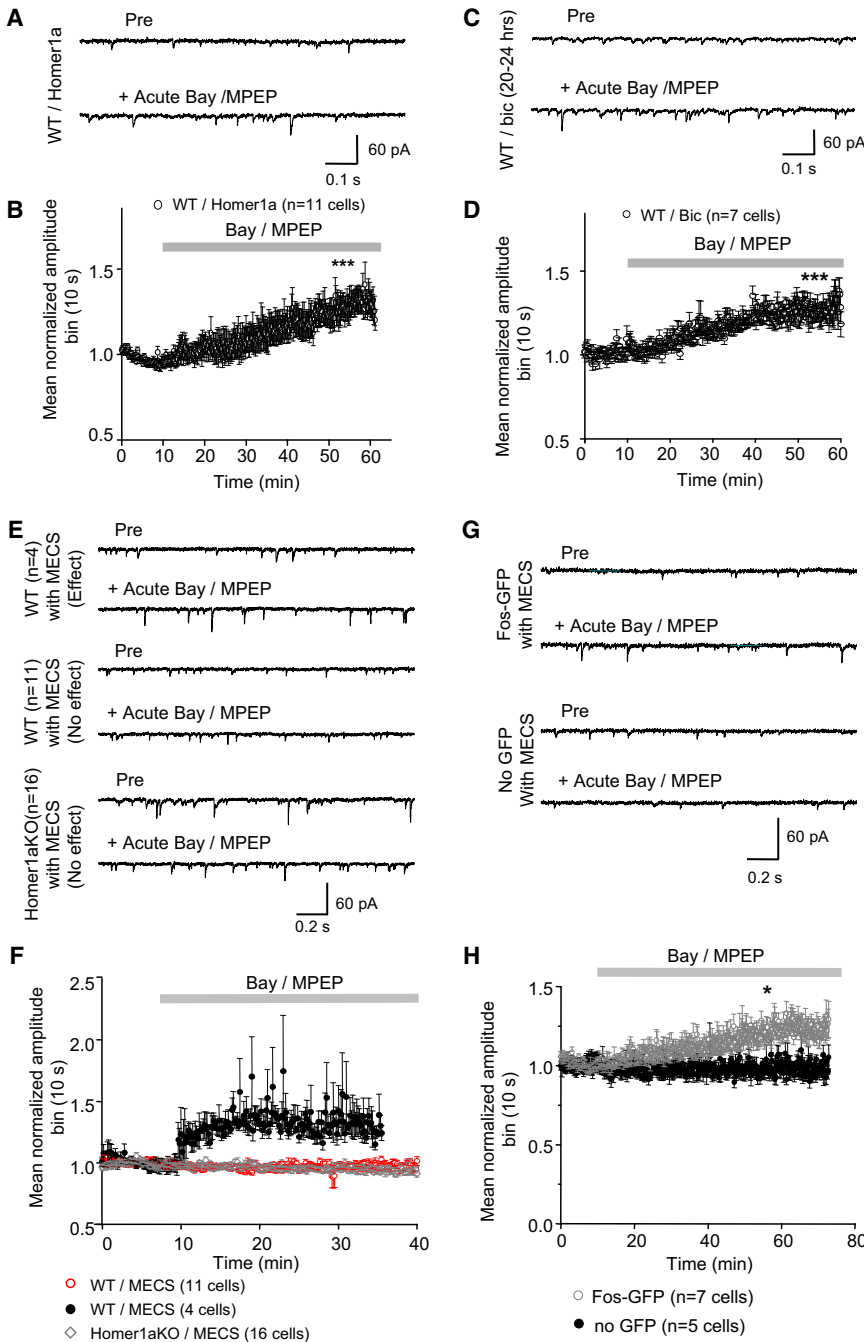
Figure 7. Homer1a Scaling of Synaptic AMPARs Is Acutely Reversed by mGluR Inverse Agonists

(A and B) Representative traces and the population time course of mEPCS recorded from WT cultured cortical neurons infected with Homer1a Sindbis virus for 8–15 hr (bin = 10 s, n = 11 cells). Acute bath application of Bay/MPEP increased mEPSC amplitude (***p < 0.001).

(C and D) WT cultured cortical neurons (n = 7 cells) were incubated for 20–24 hr with Bic. Acute bath application of Bay/MPEP increased mEPSC amplitude (***p < 0.001).

(E and F) Representative whole-cell recording traces from mice that received a single electroconvulsive seizure (MECS) 2 hr before slice preparation and were subsequently recorded within 2 hr. Bay/MPEP increased the amplitude of mEPSCs in a subset of WT neurons (n = 4 of 15 cells), but not in Homer 1a KO neurons (n = 0 of 16 cells; p < 0.05 using Fisher's exact test) (scale = 60 pA, 0.1 s, bin = 10 s).

(G and H) Representative traces and the population time course of mEPSC recorded from Fos-GFP mice that received a single electroconvulsive seizure (MECS) 2 hr before slice preparation and were subsequently recorded within 2 hr. Bay/MPEP increased the amplitude of mEPSCs in all GFP-expressing neurons (n = 7 cells), but not in neurons that did not express GFP (no GFP) (n = 5 cells; *p < 0.05).

mGluR5 are not critical for AMPAR trafficking. mGluR5 endocytosis has been reported to occur by both activity-dependent and activity-independent pathways (Dhami and Ferguson, 2006). Mechanisms that control mGluR trafficking in homeostatic scaling and the physiological significance remain to be determined.

mGluR-Dependent Scaling and Implications for Disease

Group I mGluRs are implicated in several diseases of cognition. For example, mGluR5 signaling is increased in mouse models of fragile X mental retardation syndrome (Huber et al., 2002) and may be relevant in developing therapies (Bear, 2005). Group I mGluR are considered important targets for treatment of depression, schizophrenia, and Alzheimer disease (Conn et al., 2009). Drug addiction is also dependent on mGluR5 signaling as mGluR5 KO mice show a reduced behavioral response to cocaine (Chiamulera

to WT neurons, despite the marked reduction of homeostatic changes in AMPAR. This suggests that mechanisms other than Homer1a regulate surface mGluR expression during homeostatic scaling, and that changes in surface expression of

(G) Representative traces and the population time course of mEPCS recorded from WT cultured cortical neurons infected with Homer1a Sindbis virus (n = 9 cells) or GFP Sindbis virus (n = 8 cells) for 8–15 hr (bin = 10 s). Acute bath application of Na_3VO_4 (1 mM) increases mEPSC amplitude (**p < 0.01).

(H and I) Representative traces and population time course of mEPCS recorded from WT pyramidal neurons of layer II-III prefrontal cortex in slices prepared from naive WT or Homer TKO mice. Acute bath application of Na_3VO_4 (1 mM) or Bay/MPEP increased mEPSC amplitude increase mEPSC amplitude (*p < 0.05, ***p < 0.001).

et al., 2001) and mGluR5 inverse agonists prevent self administration in monkeys (Lee et al., 2005). The present study focuses attention on the possible role of homeostatic scaling in the pathogenesis of these disorders, and identifies an important physiology to consider in the chronic use of mGluR pharmaceuticals.

EXPERIMENTAL PROCEDURES

Antibodies and Chemicals
The following antibodies were previously described or obtained commercially: mGluR1 (mouse monoclonal) from BD Biosciences; mGluR5 from Upstate; N-GluA2 from Chemicon; horse radish peroxidase (HRP) conjugated HA antibody, HRP-conjugated myc antibody, myc (mouse monoclonal) from Santa Cruz; actin (mouse monoclonal) from Sigma Aldrich. GluA2CPY was described previously (Hayashi and Huganir, 2004). Homer1, Homer2, and Homer3 were generated and described before.

The following drugs and chemicals were purchased from Tocris Biosciences: tetrodotoxin, bicuculline, Bay 36-7620, MPEP, LY367385, and (S)-MCPG, CPCCOEt.

Generation of Homer1a-Specific Knockout Mice
The Homer1a targeting construct was generated by fusing 2.7 kb of genomic DNA, including intron 4 (part thereof) and exon 5 of the Homer1 gene, with part of the rat Homer1c cDNA (2 kb), containing exons 6–10, the hGH polyadenylation site and a "floxed" Pgk-neo cassette, followed by 7.2 kb of Homer1 gene sequence. The linearized (NotI, KpnI) targeting construct was electroporated into ES ([129X1/SvJ × 129S1] F1) cells. G418 resistant ES cell clones were screened by PCR and Southern blotting for homologous recombination. Correctly targeted ES cells were injected into blastocysts, and chimeras were mated with C57BL/6 mice to produce heterozygous Homer1a knockouts.

Neuronal Culture
Neuronal cortical cultures from embryonic day 18 (E18) pups were prepared as reported previously (Rumbaugh et al., 2003), with minor alterations. For biochemistry experiments, 1×10^6 neurons were added to each well of a 6-well plate (Corning) coated with poly-L-lysine. For recording experiments, 2×10^6 neurons were added to each 60 mm dish (Corning) with coverslips coated with poly-L-lysine. Growth medium consisted of NeuroBasal (Invitrogen) supplemented with 1% fetal bovine serum (Hyclone), 2% B27, 1% Glutamax (Invitrogen), 100U/mL penicillin, and 100U/mL streptomycin (Invitrogen). Neurons were fed twice per week with glia conditioned growth medium.

Immunocytochemistry, Microscopy, and Data Analysis
Surface staining was described previously (Shepherd et al., 2006). Briefly, to label surface GluA1-containing AMPA receptors, 2.5 μg of GluA1-N JH1816 pAb was added to neuronal growth media and incubated at 10°C for 20 min. To label surface GluA2-containing AMPA receptors, 1 μg of GluA2-N Ab was added to neuronal growth media and incubated at 37°C for 15 min. The unbound excess antibody was quickly washed with fresh warmed growth medium and then fixed in 4% paraformaldehyde, 4% sucrose containing PBS solution for 20 min at 4°C. Neurons were subsequently exposed to Alexa 555 secondary antibody (1:500; Molecular Probes) and incubated at room temperature for 1 hr. After that, neurons were permeabilized with 0.2% Triton X-100 in PBS for 10 min. Coverslips were mounted on precleaned slides with PermaFluor and DABCO.

Immunofluorescence was viewed and captured using a Zeiss LSM 510 confocal laser scanning microscope using the same settings. Quantification of surface GluA1 or GluA2 puncta were carried out essentially as described (Rumbaugh et al., 2003), using Metamorph imaging software (Universal Imaging). Images were acquired and saved as multichannel TIFF files with a dynamic range of 4096 gray levels (12-bit binary; MultiTrack acquisition for confocal). To measure punctate structures, neurons were thresholded by gray value at a level close to 50% of the dynamic range. Background noise from these images was negligible. After a dendrite segment was selected, all puncta were treated as individual objects and the characteristics of each, such as pixel area, average fluorescence intensity, and total fluorescence intensity, were logged to a spreadsheet. In addition, each dendrite length was logged to calculate puncta density and total intensity per dendritic length. The average pixel intensity from each region was calculated using total intensity dividing by dendritic length and averages from all regions were derived. The average pixel intensity in each group was normalized to their control group. Significance was determined by a Student's t test.

Surface Biotinylation Assay
For surface biotinylation, drug-treated cortical neurons were cooled on ice, washed twice with ice-cold PBS++ (1× PBS, 1 mM $CaCl_2$, 0.5 mM $MgCl_2$) and then incubated with PBS++ containing 1 mg/ml Sulfo-NHS-SSBiotin (Pierce) for 30 min at 4°C. Unreacted biotin was quenched by washing cells three times with PBS++ containing 100 mM Glycine (pH 7.4) (briefly once and for 5 min twice). Cultures were harvested in RIPA buffer and sonicated. Homogenates were centrifuged at 132,000 rpm for 20 min at 4°C. Fifteen percent of the supernatant was saved as the total protein. The remaining 85% of the homogenate was rotated with Streptavidin beads (Pierce) for 2 hr. Precipitates were washed with RIPA buffer three times (5 min each time). All procedures were done at 4°C.

Slice Preparation
ECS was induced through a constant-current generator (ECT unit; Ugo Basile, Comerio, Italy) (Cole et al., 1990), in accordance with the guidelines of the Johns Hopkins Animal Care and Use Committee. The brain was dissected 2 hr after ECS and placed immediately into cold (2.5°C) modified CSF composed of the following (in mM): 110 choline chloride, 2.5 KCl, 7 $MgCl_2$, 0.5 $CaCl_2$, 2.4 Na-pyruvate, 1.3 Na-ascorbic acid, 1.2 NaH_2PO_4, 25 $NaHCO_3$, and 20 glucose. Coronal brain slices of the prefrontal cortex (250 μm) were prepared from P20-22 WT and Homer1a KO mice using a Vibratome 3000 (Leica Biosystems, St. Louis LLC, St. Louis, MO). After cutting, slices were incubated for 15 min at 32°C and then for up to 3 hr at 25°C in ACSF.

Electrophysiology
Whole-cell patch-clamp recordings from cortical cultures and slices were carried out at 30°C–32°C. Pyramidal neurons in cortical cultures and the layer II-III region of the prefrontal cortex were visually identified using Dodt Gradient Contrast. Transfected neurons were also visually identified under epifluorescence. The recording chamber was continuously perfused with artificial cerebrospinal fluid (ACSF) containing (in mM): 124 NaCl, 2.5 KCl, 1.3 $MgCl_2$, 2.5 $CaCl_2$, 1 NaH_2PO_4, 26.2 $NaHCO_3$, and 10 glucose, equilibrated with 95% O_2 and 5% CO_2 (pH 7.4, 305 ± 5 mmol/kg). The bath solution also contained both 1 μM TTX and 10 μM GABAzine to block action potential dependent EPSCs and $GABA_A$ receptors, respectively. The pipette solution contained (in mM): 90 Cs-methansulfonate, 48.5 CsCl, 5 ethylene glycol tetraacetic acid, 2 $MgCl_2$, 2 Na-ATP, 0.4 Na-GTP, and 5 HEPES (pH 7.2, 290 ± 2 mmol/kg). Patch pipettes were pulled from borosilicate glass (4–5 MΩ) using a horizontal puller (Sutter Instruments, Novato, CA). Signals were recorded with a Multiclamp 700B (Molecular Devices, Union City, CA) amplifier, filtered at 2 kHz and sampled at 10 kHz. To detect a sufficient number of events (200 events per neuron), recordings were performed on gap free mode (sweeps of 30 s without any latency). Data were acquired 3 min after achieving the whole-cell configuration. Series resistances (Rs) of recordings ranged between 10 and 15 MΩ. Cells were rejected from analysis if Rs changed by more than 15%. mEPSCs were analyzed by Mini Analysis Software (Synaptosoft, NJ). All group data are shown as mean ± standard error of the mean (SEM). Statistical comparison was performed by the independent t test, ANOVA for multiple comparison (see Figures 1F and 5G), or Fisher's exact test (see Figure 7F). All drugs were purchased from Tocris (Ellisville, MO) except for TTX (Ascent Scientific LLC, Princeton, NJ).

Statistical Analysis
All the data were analyzed by two-tailed Student's t test except the analysis of the multiple comparisons (Figures 1F and 5G). Error bars indicate the SEM.

REFERENCES

Ahmadian, G., Ju, W., Liu, L., Wyszynski, M., Lee, S.H., Dunah, A.W., Taghibiglou, C., Wang, Y., Lu, J., Wong, T.P., et al. (2004). Tyrosine phosphorylation of GluR2 is required for insulin-stimulated AMPA receptor endocytosis and LTD. EMBO J. *23*, 1040–1050.

Ango, F., Prezeau, L., Muller, T., Tu, J.C., Xiao, B., Worley, P.F., Pin, J.P., Bockaert, J., and Fagni, L. (2001). Agonist-independent activation of metabotropic glutamate receptors by the intracellular protein Homer. Nature *411*, 962–965.

Ango, F., Robbe, D., Tu, J.C., Xiao, B., Worley, P.F., Pin, J.P., Bockaert, J., and Fagni, L. (2002). Homer-dependent cell surface expression of metabotropic glutamate receptor type 5 in neurons. Mol. Cell. Neurosci. *20*, 323–329.

Barnes, C.A., Jung, M.W., McNaughton, B.L., Korol, D.L., Andreasson, K., and Worley, P.F. (1994). LTP saturation and spatial learning disruption: Effects of task variables and saturation levels. J. Neurosci. *14*, 5793–5806.

Barth, A.L., Gerkin, R.C., and Dean, K.L. (2004). Alteration of neuronal firing properties after in vivo experience in a FosGFP transgenic mouse. J. Neurosci. *24*, 6466–6475.

Bear, M.F. (2005). Therapeutic implications of the mGluR theory of fragile X mental retardation. Genes Brain Behav. *4*, 393–398.

Brakeman, P.R., Lanahan, A.A., O'Brien, R., Roche, K., Barnes, C.A., Huganir, R.L., and Worley, P.F. (1997). Homer: A protein that selectively binds metabotropic glutamate receptors. Nature *386*, 284–288.

Brock, C., Oueslati, N., Soler, S., Boudier, L., Rondard, P., and Pin, J.P. (2007). Activation of a dimeric metabotropic glutamate receptor by intersubunit rearrangement. J. Biol. Chem. *282*, 33000–33008.

Chiamulera, C., Epping-Jordan, M.P., Zocchi, A., Marcon, C., Cottiny, C., Tacconi, S., Corsi, M., Orzi, F., and Conquet, F. (2001). Reinforcing and locomotor stimulant effects of cocaine are absent in mGluR5 null mutant mice. Nat. Neurosci. *4*, 873–874.

Chowdhury, S., Shepherd, J.D., Okuno, H., Lyford, G., Petralia, R.S., Plath, N., Kuhl, D., Huganir, R.L., and Worley, P.F. (2006). Arc/Arg3.1 interacts with the endocytic machinery to regulate AMPA receptor trafficking. Neuron *52*, 445–459.

Cole, A.J., Abu-Shakra, S., Saffen, D.W., Baraban, J.M., and Worley, P.F. (1990). Rapid rise in transcription factor mRNAs in rat brain after electroshock-induced seizures. J. Neurochem. *55*, 1920–1927.

Conn, P.J., Christopoulos, A., and Lindsley, C.W. (2009). Allosteric modulators of GPCRs: A novel approach for the treatment of CNS disorders. Nat. Rev. Drug Discov. *8*, 41–54.

Dan, Y., and Poo, M.M. (2004). Spike timing-dependent plasticity of neural circuits. Neuron *44*, 23–30.

Dhami, G.K., and Ferguson, S.S. (2006). Regulation of metabotropic glutamate receptor signaling, desensitization and endocytosis. Pharmacol. Ther. *111*, 260–271.

Feng, W., Tu, J., Yang, T., Vernon, P.S., Allen, P.D., Worley, P.F., and Pessah, I.N. (2002). Homer regulates gain of ryanodine receptor type 1 channel complex. J. Biol. Chem. *277*, 44722–44730.

Gladding, C.M., Collett, V.J., Jia, Z., Bashir, Z.I., Collingridge, G.L., and Molnar, E. (2009). Tyrosine dephosphorylation regulates AMPAR internalisation in mGluR-LTD. Mol. Cell. Neurosci. *40*, 267–279.

Hayashi, T., and Huganir, R.L. (2004). Tyrosine phosphorylation and regulation of the AMPA receptor by SRC family tyrosine kinases. J. Neurosci. *24*, 6152–6160.

Huber, K.M., Gallagher, S.M., Warren, S.T., and Bear, M.F. (2002). Altered synaptic plasticity in a mouse model of fragile X mental retardation. Proc. Natl. Acad. Sci. USA *99*, 7746–7750.

Kammermeier, P.J. (2008). Endogenous homer proteins regulate metabotropic glutamate receptor signaling in neurons. J. Neurosci. *28*, 8560–8567.

Kingston, A.E., Ornstein, P.L., Wright, R.A., Johnson, B.G., Mayne, N.G., Burnett, J.P., Belagaje, R., Wu, S., and Schoepp, D.D. (1998). LY341495 is a nanomolar potent and selective antagonist of group II metabotropic glutamate receptors. Neuropharmacology *37*, 1–12.

Kitano, J., Nishida, M., Itsukaichi, Y., Minami, I., Ogawa, M., Hirano, T., Mori, Y., and Nakanishi, S. (2003). Direct interaction and functional coupling between metabotropic glutamate receptor subtype 1 and voltage-sensitive Cav2.1 Ca2+ channel. J. Biol. Chem. *278*, 25101–25108.

Lee, B., Platt, D.M., Rowlett, J.K., Adewale, A.S., and Spealman, R.D. (2005). Attenuation of behavioral effects of cocaine by the metabotropic glutamate receptor 5 antagonist 2-methyl-6-(phenylethynyl)-pyridine in squirrel monkeys: Comparison with dizocilpine. J. Pharmacol. Exp. Ther. *312*, 1232–1240.

Lyford, G.L., Yamagata, K., Kaufmann, W.E., Barnes, C.A., Sanders, L.K., Copeland, N.G., Gilbert, D.J., Jenkins, N.A., Lanahan, A.A., and Worley, P.F. (1995). Arc, a growth factor and activity-regulated gene, encodes a novel cytoskeleton-associated protein that is enriched in neuronal dendrites. Neuron *14*, 433–445.

Maejima, T., Hashimoto, K., Yoshida, T., Aiba, A., and Kano, M. (2001). Presynaptic inhibition caused by retrograde signal from metabotropic glutamate to cannabinoid receptors. Neuron *31*, 463–475.

Makino, H., and Malinow, R. (2009). AMPA receptor incorporation into synapses during LTP: The role of lateral movement and exocytosis. Neuron *64*, 381–390.

Matthews, C.C., Zielke, H.R., Wollack, J.B., and Fishman, P.S. (2000). Enzymatic degradation protects neurons from glutamate excitotoxicity. J. Neurochem. *75*, 1045–1052.

Milligan, G. (2003). Constitutive activity and inverse agonists of G protein-coupled receptors: A current perspective. Mol. Pharmacol. *64*, 1271–1276.

Mizutani, A., Kuroda, Y., Futatsugi, A., Furuichi, T., and Mikoshiba, K. (2008). Phosphorylation of Homer3 by calcium/calmodulin-dependent kinase II regulates a coupling state of its target molecules in Purkinje cells. J. Neurosci. *28*, 5369–5382.

O'Hara, P.J., Sheppard, P.O., Thogersen, H., Venezia, D., Haldeman, B.A., McGrane, V., Houamed, K.M., Thomsen, C., Gilbert, T.L., and Mulvihill, E.R. (1993). The ligand-binding domain in metabotropic glutamate receptors is related to bacterial periplasmic binding proteins. Neuron *11*, 41–52.

Oliet, S.H., Malenka, R.C., and Nicoll, R.A. (1997). Two distinct forms of long-term depression coexist in CA1 hippocampal pyramidal cells. Neuron *18*, 969–982.

Pagano, A., Ruegg, D., Litschig, S., Stoehr, N., Stierlin, C., Heinrich, M., Floersheim, P., Prezeau, L., Carroll, F., Pin, J.P., et al. (2000). The non-competitive antagonists 2-methyl-6-(phenylethynyl)pyridine and 7-hydroxyiminocyclopropan[b]chromen-1a-carboxylic acid ethyl ester interact with overlapping binding pockets in the transmembrane region of group I metabotropic glutamate receptors. J. Biol. Chem. *275*, 33750–33758.

Park, S., Park, J.M., Kim, S., Kim, J.A., Shepherd, J.D., Smith-Hicks, C.L., Chowdhury, S., Kaufmann, W., Kuhl, D., Ryazanov, A.G., et al. (2008). Elongation factor 2 and fragile X mental retardation protein control the dynamic translation of Arc/Arg3.1 essential for mGluR-LTD. Neuron *59*, 70–83.

Pula, G., Mundell, S.J., Roberts, P.J., and Kelly, E. (2004). Agonist-independent internalization of metabotropic glutamate receptor 1a is arrestin- and clathrin-dependent and is suppressed by receptor inverse agonists. J. Neurochem. 89, 1009–1020.

Rumbaugh, G., Sia, G.M., Garner, C.C., and Huganir, R.L. (2003). Synapse-associated protein-97 isoform-specific regulation of surface AMPA receptors and synaptic function in cultured neurons. J. Neurosci. 23, 4567–4576.

Shepherd, J.D., Rumbaugh, G., Wu, J., Chowdhury, S., Plath, N., Kuhl, D., Huganir, R.L., and Worley, P.F. (2006). Arc/Arg3.1 mediates homeostatic synaptic scaling of AMPA receptors. Neuron 52, 475–484.

Snyder, E.M., Philpot, B.D., Huber, K.M., Dong, X., Fallon, J.R., and Bear, M.F. (2001). Internalization of ionotropic glutamate receptors in response to mGluR activation. Nat. Neurosci. 4, 1079–1085.

Tu, J.C., Xiao, B., Yuan, J.P., Lanahan, A.A., Leoffert, K., Li, M., Linden, D.J., and Worley, P.F. (1998). Homer binds a novel proline-rich motif and links group 1 metabotropic glutamate receptors with IP3 receptors. Neuron 21, 717–726.

Turrigiano, G.G. (2008). The self-tuning neuron: Synaptic scaling of excitatory synapses. Cell 135, 422–435.

Turrigiano, G.G., and Nelson, S.B. (2000). Hebb and homeostasis in neuronal plasticity. Curr. Opin. Neurobiol. 10, 358–364.

Waung, M.W., Pfeiffer, B.E., Nosyreva, E.D., Ronesi, J.A., and Huber, K.M. (2008). Rapid translation of Arc/Arg3.1 selectively mediates mGluR-dependent LTD through persistent increases in AMPAR endocytosis rate. Neuron 59, 84–97.

Xiong, C., Levis, R., Shen, P., Schlesinger, S., Rice, C.M., and Huang, H.V. (1989). Sindbis virus: An efficient, broad host range vector for gene expression in animal cells. Science 243, 1188–1191.

Yuan, J.P., Kiselyov, K., Shin, D.M., Chen, J., Shcheynikov, N., Kang, S.H., Dehoff, M.H., Schwarz, M.K., Seeburg, P.H., Muallem, S., and Worley, P.F. (2003). Homer binds TRPC family channels and is required for gating of TRPC1 by IP3 receptors. Cell 114, 777–789.

Zhang, Y., Venkitaramani, D.V., Gladding, C.M., Zhang, Y., Kurup, P., Molnar, E., Collingridge, G.L., and Lombroso, P.J. (2008). The tyrosine phosphatase STEP mediates AMPA receptor endocytosis after metabotropic glutamate receptor stimulation. J. Neurosci. 28, 10561–10566.